An oceanic origin for the increase of atmospheric radiocarbon during the Younger Dryas

Article

Published Version

An oceanic origin for the increase of atmospheric radiocarbon during the Younger Dryas

Joy S. Singarayer,[1] David A. Richards,[1] Andy Ridgwell,[1] Paul J. Valdes,[1] William E. N. Austin,[2] and J. Warren Beck[3]

Received 20 March 2008; revised 5 May 2008; accepted 28 May 2008; published 26 July 2008.

[1] Variations in carbon-14 to carbon-12 ratio in the atmosphere ($\Delta^{14}C_{atm}$) provide a powerful diagnostic for elucidating the timing and nature of geophysical and anthropological change. The (Atlantic) marine archive suggests a rapid $\Delta^{14}C_{atm}$ increase of 50‰ at the onset of the Younger Dryas (YD) cold reversal (12.9–11.7 kyr BP), which has not yet been satisfactorily explained in terms of magnitude or causal mechanism, as either a change in ocean ventilation or production rate. Using Earth-system model simulations and comparison of marine-based radiocarbon records from different ocean basins, we demonstrate that the YD $\Delta^{14}C_{atm}$ increase is smaller than suggested by the marine archive. This is due to changes in reservoir age, predominantly caused by reduced ocean ventilation. **Citation:** Singarayer, J. S., D. A. Richards, A. Ridgwell, P. J. Valdes, W. E. N. Austin, and J. W. Beck (2008), An oceanic origin for the increase of atmospheric radiocarbon during the Younger Dryas, *Geophys. Res. Lett.*, *35*, L14707, doi:10.1029/2008GL034074.

1. Introduction

[2] Variation in $\Delta^{14}C_{atm}$ is linked to climatic fluctuations, which affect the distribution of ^{14}C throughout the Earth system, and to changes in geomagnetic and solar magnetic field intensity, which affects the production rate of ^{14}C. While we are able to draw upon dendrochronology for $\Delta^{14}C_{atm}$ after 12.4 kyr BP [*Friedrich et al.*, 2004], prior to this we must rely on less well-constrained data mainly from marine archives, such as corals [*Fairbanks et al.*, 2005] and foraminifera [*Hughen et al.*, 2000]. Marine reconstructions assume a constant difference between the ^{14}C age of the ocean and that of the contemporaneous atmosphere (the reservoir age, R) to calculate $\Delta^{14}C_{atm}$. A range of temporally invariant values of R, usually between 300 and 450 yr, have been assumed for marine $\Delta^{14}C_{atm}$ reconstructions from different locations in the ocean. However, marine R can vary temporally and spatially as a result of atmospheric production rate or ocean ventilation changes [*Butzin et al.*, 2005; *Bondevik et al.*, 2006; *Delaygue et al.*, 2003]. Indeed, comparison of tropical Atlantic data with a floating tree-ring record [*Kromer et al.*, 2004] suggests a decrease in R of ~200 years at the YD onset. Here, we use an Earth system model of intermediate complexity to examine the constant-R assumption, and reliability of ^{14}C age calibration based on marine archives. In doing so, we explore potential causes of apparent variations in the marine radiocarbon record.

[3] We focus on a critical period that interrupted the last deglaciation: the Younger Dryas (YD; 12.9–11.7 kyr BP) cold reversal. According to $\Delta^{14}C_{atm}$ reconstructions [*Reimer et al.*, 2004; *Fairbanks et al.*, 2005; *Hughen et al.*, 2000], a large positive $\Delta^{14}C_{atm}$ excursion occurred at the start of the YD (Figure 1a). Hughen et al. estimate an apparent increase of ~50‰. The cause of this peak, and indeed the nature of Earth system change across the globe during this period are keenly debated [*Goslar et al.*, 2000; *Marchal et al.*, 2001]. This apparent excursion reached a peak $\Delta^{14}C_{atm}$ value within 200 years of onset, and started concurrently with the initiation of cool Northern Hemisphere temperatures at the Bölling-Allerød/YD transition, as inferred from $\delta^{18}O$ in ice cores [*Rasmussen et al.*, 2006] (Figure 1b). Two key issues are: (1) the structure and amplitude of the $\Delta^{14}C_{atm}$ anomaly in the absence of direct estimates of the atmospheric signal, and (2) the extent to which the $\Delta^{14}C_{atm}$ anomaly can be attributed to changes in the production rate due to solar/geomagnetic variation and/or abrupt changes in Atlantic overturning, which influences atmosphere-ocean carbon exchange.

[4] The flux of the cosmogenic nuclide ^{10}Be (Figure 1d) can be used as a proxy for production rate [*Muscheler et al.*, 2004] because it is influenced by solar and geomagnetic intensity but, unlike ^{14}C, is relatively unaffected by redistribution within the Earth system during changing climate conditions. Current ^{10}Be records show no obvious excursion at the beginning of the YD, although uncertainties in ice accumulation rates [*Muscheler et al.*, 2004] used to calculate ^{10}Be production rate from ^{10}Be concentration may mask variation. Alternatively, Pa/Th data from the North Atlantic provide evidence for reduced North Atlantic Deep Water (NADW) formation during the YD [*McManus et al.*, 2004] which could affect $\Delta^{14}C_{atm}$ via the associated reorganization of carbon reservoirs. Although Earth system models have previously simulated a $\Delta^{14}C_{atm}$ increase in response to surface freshwater "hosing' and shutdown of NADW formation [*Marchal et al.*, 2001; *Butzin et al.*, 2005], they have significantly underestimated the apparent magnitude and rate of YD $\Delta^{14}C_{atm}$ increase as derived from marine records.

[5] In this study, we examine the modelled spatial and temporal distribution of ^{14}C within the various reservoirs of the global carbon cycle in response to both meltwater input and increased cosmogenic production using the GENIE-1 (Grid ENabled Integrated Earth system) intermediate-

[1]School of Geographical Sciences, University of Bristol, Bristol, UK.
[2]School of Geography and Geosciences, St. Andrews University, St. Andrews, UK.
[3]NSF-AMS Laboratory, Department of Physics, University of Arizona, Tucson, Arizona, USA.

0094-8276/08/2008GL034074

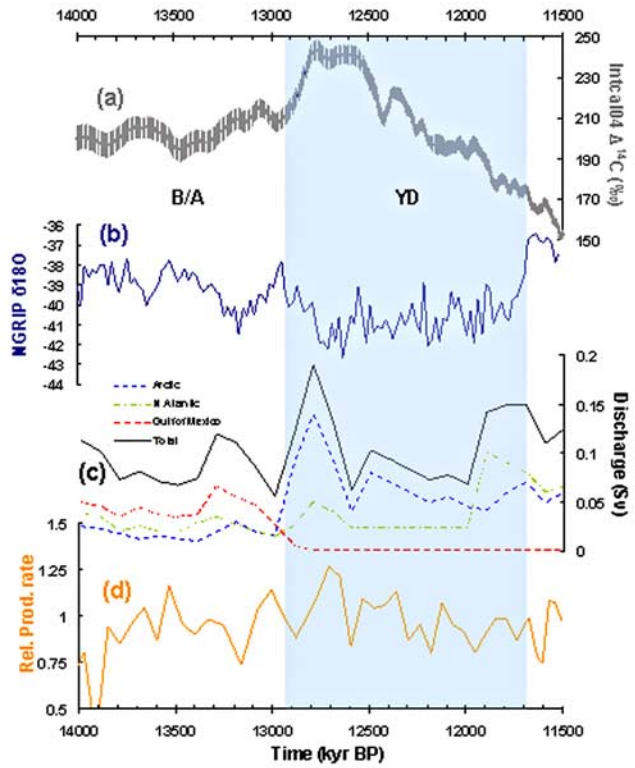

Figure 1. Comparison of various paleo-records from the end of the Bölling-Allerød through the Younger Dryas. (a) Intcal04 $\Delta^{14}C_{atm}$ [*Reimer et al.*, 2004], (b) $\delta^{18}O$ from the GISP2 ice core [*Rasmussen et al.*, 2006], (c) reconstructed melt-water discharge into the Arctic/Atlantic [*Tarasov and Peltier*, 2005], and (d) radiocarbon production rate relative to present, derived from GISPII ^{10}Be [*Muscheler et al.*, 2004].

complexity model [*Lenton et al.*, 2006]. The results were compared to empirical records to investigate the cause of the YD $\Delta^{14}C_{atm}$ increase.

2. Model and Simulations

[6] GENIE-1 consists of a dynamic 3-D ocean, 2-D energy and moisture balance atmosphere, sea-ice, and terrestrial, ocean, and sediment carbon cycle components, on a 36 by 36 equal area grid with 16 vertical ocean levels [*Lenton et al.*, 2006; *Ridgwell et al.*, 2007; *Ridgwell and Hargreaves*, 2007]. It is forced with the annual average wind speed [*Trenberth et al.*, 1989] and calibrated against present-day observations of surface air temperature and humidity, and 3D ocean temperature and salinity using a multi-objective tuning process [*Price et al.*, 2006].

[7] For idealised Younger Dryas simulations, the model was prescribed with fixed ice sheet [*Peltier*, 1994] and orbital boundary conditions for 13 kyr BP. The model was first spun up for 40 kyr with a prescribed CO_2 concentration of 237 ppm and ^{14}C production rate to produce $\Delta^{14}C_{atm}$ of 210‰. A resulting AMOC maximum of 15.9 Sv and annual average SST of 14.8°C were obtained. During the actual Younger Dryas simulations, CO_2, ^{13}C and ^{14}C concentrations are predicted by the interactions between terrestrial, marine, and sediment carbon cycling and weathering.

[8] Firstly, the model was forced with an idealised freshwater flux in the high latitude Atlantic Ocean (Scenario A, Figure 2a), consistent with reconstructions of meltwater/iceberg discharge into the Atlantic and Arctic Ocean (Figure 1c) [*Tarasov and Peltier*, 2005] and equivalent to 7 m sea level rise in total, which is within the range of estimates from palaeo-records for the YD period [*Fleming et al.*, 1998]. A second simulation was conducted in which an instantaneous increase in ^{14}C production of 25% is prescribed for 400 yr (Scenario B, Figure 2a), which is the maximum magnitude of increase that could potentially be inferred from the ^{10}Be record within uncertainties, to

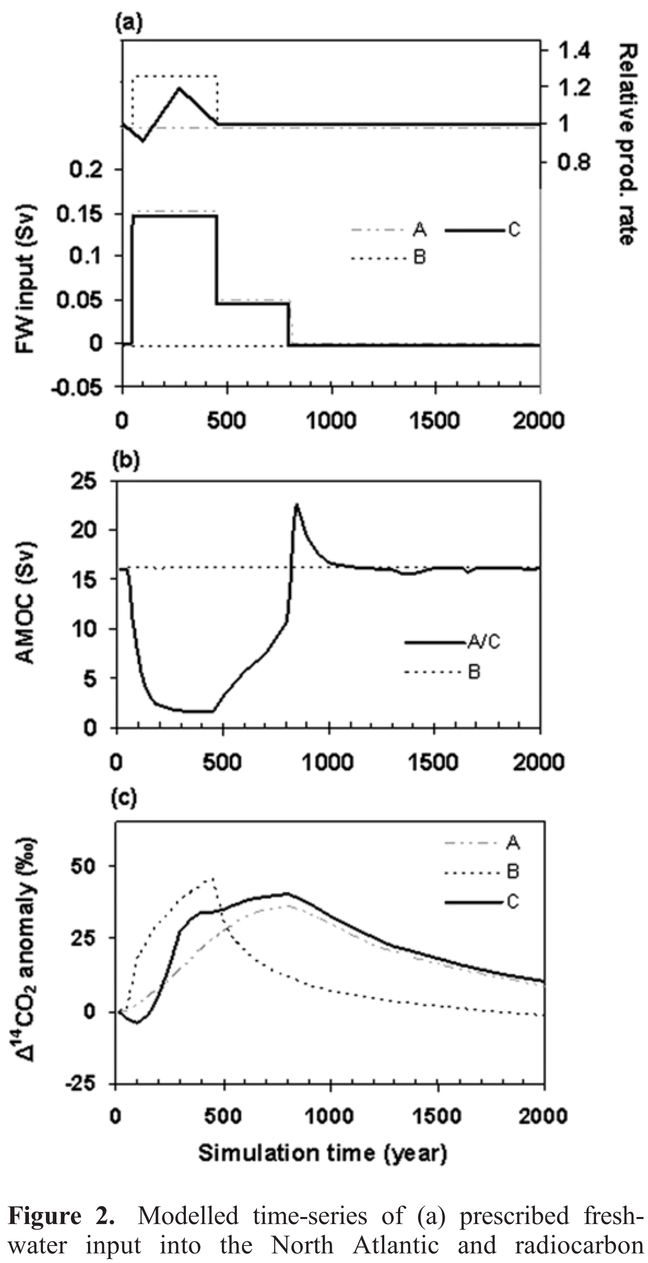

Figure 2. Modelled time-series of (a) prescribed freshwater input into the North Atlantic and radiocarbon production rate for: scenario A (freshwater only), scenario B (production rate only), and scenario C (freshwater and production rate), (b) Atlantic meridional overturning circulation index, which is defined here as the maximum value between 0–90°N at depth >1200 m, and (c) change in global mean $\Delta^{14}C_{atm}$.

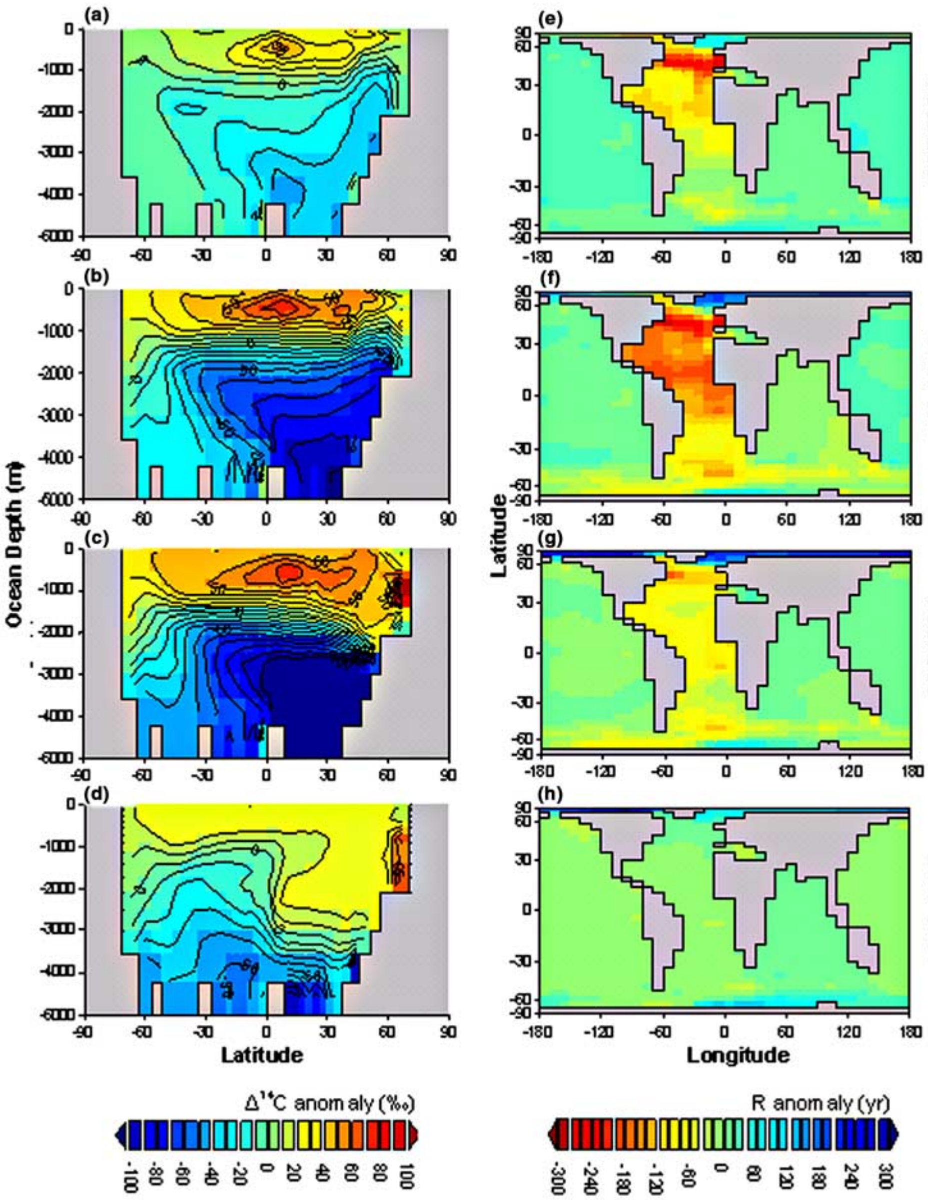

Figure 3. Changes in (a–d) model annual Atlantic zonally-averaged dissolved inorganic Δ^{14}C and (3–h) surface reservoir age, R, for model scenario A at years 200, 450, 800 and 1000.

evaluate the response solely to production rate variation. In addition, a simulation was performed in which both a shutdown of NADW and idealised transient changes in production rate were prescribed, based on the increase in ^{14}C production at the start of the YD derived from ^{10}Be ice-core data (Scenario C, Figure 2a).

3. Model Results

[9] In scenario A, freshwater input is sufficient to shutdown NADW in the model, which takes ~100 yr (Figure 2b). This produces an increase in $\Delta^{14}C_{atm}$ of 30‰ over 800 yr (Figure 2c). The rate of $\Delta^{14}C_{atm}$ increase is similar to that predicted in previous modelling studies [*Marchal et al.*, 2001; *Butzin et al.*, 2005]. However, this is significantly slower than the marine reconstructions apparently indicate (Figure 1a). Introducing a 25% increase in ^{14}C production rate without freshwater-hosing (scenario B), generates a more rapid increase in $\Delta^{14}C_{atm}$ (Figure 2c) more comparable with marine-reconstructed $\Delta^{14}C_{atm}$ than the freshwater flux simulations. The final simulation (scenario C), which prescribed both freshwater-hosing and production rate changes, yielded $\Delta^{14}C_{atm}$ increases of the same order as the other hosing experiments (~40‰), but with a more rapid increase in $\Delta^{14}C_{atm}$ than hosing alone.

[10] Reduction in ocean ventilation due to NADW shutdown (A) enables a longer period for exchange of ^{14}C between atmosphere and Atlantic surface water. This results in surface water Δ^{14}C values that are closer to the values in the atmosphere, and consequently lower R (Figure 3). Large reductions in R occur in the North Atlantic by year 200 (Figure 3e–3h). By model year 450 there is a considerable decrease in R over the whole of the Atlantic Ocean of up to 300 yr. Conversely, an increase in R is observed under

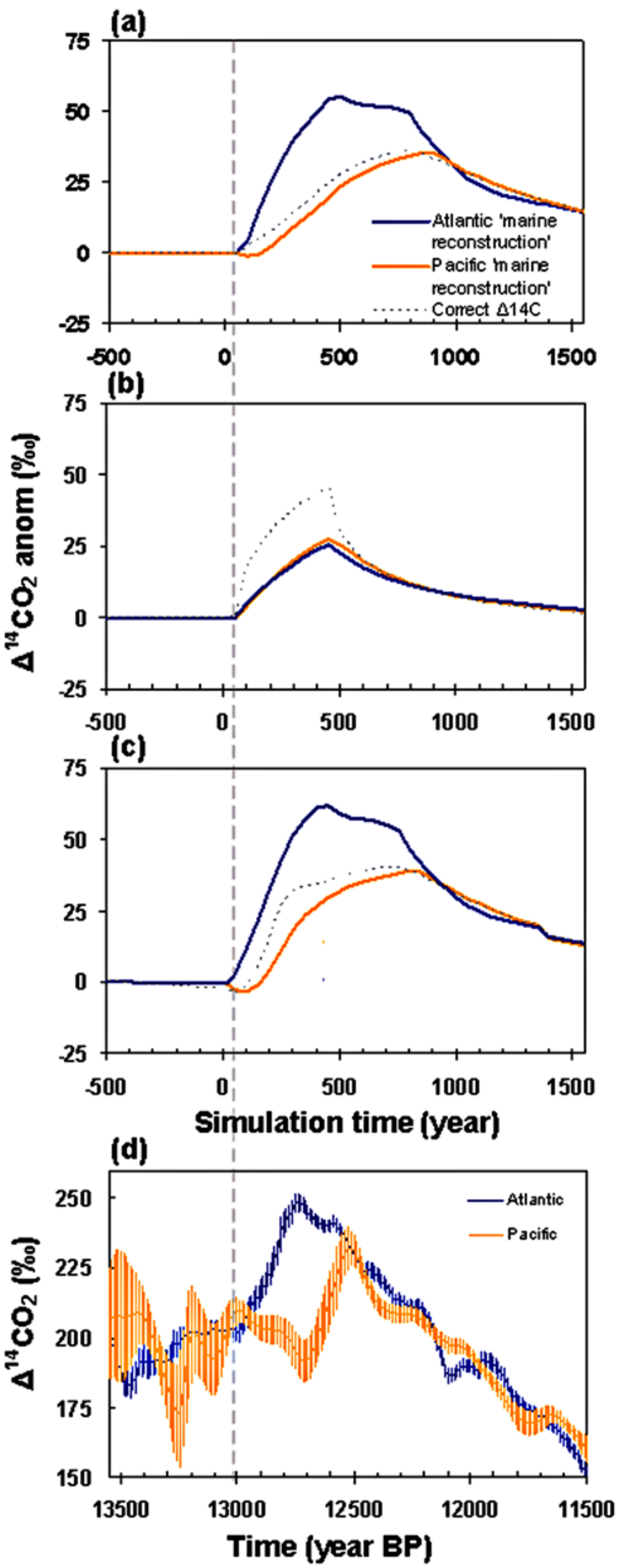

Figure 4. (a) Model transient atmospheric changes in $\Delta^{14}C$ (dotted line) for model scenario A, compared with reconstructions derived from Atlantic (blue) and Pacific (orange) surface ocean modelled DIC $\Delta^{14}C$, assuming an artificially constant reservoir age of 400 yr following *Hughen et al.* [2000], (b) same as Figure 4a but for model scenario B, (c) same as Figure 4a but for model scenario C, and (d) marine-based data were separated into those from Atlantic and Pacific sectors. These data were averaged and smoothed to form the $\Delta^{14}C$ records shown. The dashed grey line represents the start of the modelled freshwater input. The raw data are shown in supplementary material, Figure S4.

regions such as the Arctic Ocean, where sea-ice extent is greater and, hence, air-sea gas exchange is reduced. The increase in R in the Arctic and North Atlantic is of the same order of magnitude as that seen in ocean core records [*Bondevik et al.*, 2006]. Much smaller increases in R are modelled in the Pacific. This heterogeneous spatial distribution of R in scenario A is in contrast to that produced by an increase in ^{14}C production rate, which produces a more uniform increase in R of up to 200 yr in both the Atlantic and Pacific (scenario B; not shown).

4. Model-Data Comparison

[11] Given the significant transient and spatial changes in modelled R, we next considered the implications for the robustness of the marine-based $\Delta^{14}C_{atm}$ data reconstructions (which assume a constant R) at the YD onset. Using the original simulations A and B, we produced modelled time-series of ^{14}C concentrations for the surface ocean in the same regions of the tropical Atlantic and Pacific as the paleo-archive (supplementary material, Figure S1[1]) and use these to reconstruct $\Delta^{14}C_{atm}$ by subtracting a value for R that is (wrongly) assumed to be constant [e.g., *Delaygue et al.*, 2003]. When a constant R is imposed on the tropical Atlantic model surface ocean concentrations, the freshwater-hosing-only simulation results in an artificially large increase in reconstructed $\Delta^{14}C_{atm}$, which reaches a maximum value several hundred years before the model maximum $\Delta^{14}C_{atm}$ (Figure 4a). When the constant-R reconstruction is performed on modelled Pacific surface ocean Δ^{14}C, there is a significant delay before the rise in reconstructed $\Delta^{14}C_{atm}$ begins (Figure 4a). In contrast to this, scenario B (^{14}C production rate increase only), produces $\Delta^{14}C_{atm}$ reconstructions that are damped in both the Pacific and Atlantic in comparison to the atmospheric values of $\Delta^{14}C_{atm}$ (Figure 4b), and leads (Atlantic) and lags (Pacific) are not seen. In the production+hosing scenario (C), constant-R $\Delta^{14}C_{atm}$ reconstructions (Figure 4c) produce a similar lead/lag pattern as Figure 4a, indicating the dominating effect of the change in ocean ventilation.

[12] To evaluate whether the phase and amplitude effects described above were present in the $\Delta^{14}C_{atm}$ record, we compared smoothed marine-based $\Delta^{14}C_{atm}$ records using data from the Atlantic [*Fairbanks et al.*, 2005; *Hughen et al.*, 2000] and Pacific [*Fairbanks et al.*, 2005; *Cutler et al.*, 2004; *Burr et al.*, 2004] (Figure 4d). There is general agreement between the two ocean basins prior to the YD and during the latter half of the YD. however, at the start of the YD, the maximum $\Delta^{14}C_{atm}$ occurs ~300 yr earlier in the Atlantic reconstruction than the Pacific reconstruction, and is significantly larger. This pattern is comparable to the modelled scenario A (Figures 4a and 4c), and indicates that a decrease in Atlantic basin ventilation is the dominant contributing factor to the initial rise in reconstructed $\Delta^{14}C_{atm}$.

[13] Additional support for the model results is provided by a previous comparison of a floating tree ring record [*Kromer et al.*, 2004] with the Cariaco Basin varved sediment $\Delta^{14}C_{atm}$ record. Discrepancies between them suggested that reservoir ages in the Cariaco Basin (located in the Atlantic) decreased by ~200 yr during the early part of the Younger Dryas, as found in our model simulations of the tropical Atlantic (Figure 3f).

[1]Auxiliary materials are available in the HTML. doi:10.1029/2008GL034074.

5. Conclusions

[14] We demonstrate here that comparisons between marine ^{14}C data from different oceans and Earth-system model simulations of Younger Dryas conditions can elucidate the mechanisms ^{14}C variations. We find that the Younger Dryas $\Delta^{14}C_{atm}$ increase is predominantly caused by ocean reorganisation rather than changes in production rate.

[15] For the first time, the possibility exists for reconciling empirical marine and modelled data for this period, and for understanding the causes of other variations in the radiocarbon record. Using our model-data comparison strategy, we conclude that marine-derived $\Delta^{14}C_{atm}$ reconstructions that assume temporally invariant reservoir ages will yield erroneous phase relationships and amplitudes during other periods of rapid change in ocean overturning or ^{14}C production that have occurred in the last 50 kyr. This has implications for the accuracy of the ^{14}C age calibration efforts based on marine archives. However, there is potential for model simulations to inform and improve the error estimation of marine-based reconstructions of atmospheric radiocarbon abundance.

[16] **Acknowledgments.** JSS was funded by NERC. We would like to thank Louise Brown for initial discussions. WENA acknowledges funding support from the NERC RAPID project.

References

Bondevik, S., J. Mangerud, H. H. Birks, S. Gulliksen, and P. Reimer (2006), Changes in North Atlantic radiocarbon reservoir ages during the Allerød and Younger Dryas, *Science*, *312*, 1514–1517.

Burr, G. S., C. Galang, F. W. Taylor, C. Gallup, R. L. Edwards, K. Cutler, and B. Quirk (2004), Radiocarbon results from a 13-kyr BP coral from the Huon Peninsula, Papua New Guinea, *Radiocarbon*, *46*(3), 1211–1224.

Butzin, M., M. Prange, and G. Lohmann (2005), Radiocarbon simulations for the glacial ocean: The effects of wind stress, Southern Ocean sea ice and Heinrich events, *Earth Planet. Sci. Lett.*, *235*, 45–61.

Cutler, K. B., S. C. Gray, G. S. Burr, R. L. Edwards, F. W. Taylor, G. Cabioch, J. W. Beck, H. Cheng, and J. Moore (2004), Radiocarbon calibration and comparison to 50 kyr BP with paired ^{14}C and ^{230}Th dating of corals from Vanuatu and Papua New Guinea, *Radiocarbon*, *46*(3), 1127–1160.

Delaygue, G., T. F. Stocker, F. Joos, and G.-K. Plattner (2003), Simulation of atmospheric radiocarbon during abrupt oceanic circulation changes: Trying to reconcile models and reconstructions, *Quat. Sci. Rev.*, *22*, 1647–1658.

Fairbanks, R. G., R. A. Mortlock, T.-C. Chiu, L. Cao, A. Kaplan, T. P. Guilderson, T. W. Fairbanks, A. L. Bloom, P. M. Grootes, and M.-J. Nadeau (2005), Radiocarbon calibration curve spanning 0 to 50,000 years BP based on paired ^{230}Th/^{234}U/^{238}U and ^{14}C dates on pristine corals, *Quat. Sci. Rev.*, *24*, 1781–1796.

Fleming, K., P. Johnston, D. Zwartz, Y. Yokoyama, K. Lambeck, and J. Chappell (1998), Refining the eustatic sea-level curve since the Last Glacial Maximum using far- and intermediate-field sites, *Earth Planet. Sci. Lett.*, *163*, 327–342.

Friedrich, M., S. Remmelel, B. Kromer, J. Hofmann, M. Spurk, K. F. Kaiser, C. Orcel, and M. Kuppers (2004), The 12,460-year Hohenheim oak and pine tree-ring chronology from central Europe—A unique annual record for radiocarbon calibration and paleoenvironment reconstructions, *Radiocarbon*, *46*(3), 1111–1122.

Goslar, T., M. Arnold, N. Tisnerat-Laborde, J. Czernik, and K. Wiêckowski (2000), Variations of Younger Dryas atmospheric radiocarbon explicable without ocean circulation changes, *Nature*, *403*, 877–880.

Hughen, K. A., J. R. Southon, S. J. Lehman, and J. T. Overpeck (2000), Synchronous radiocarbon and climate shifts during the last deglaciation, *Science*, *290*, 1951–1954.

Kromer, B., M. Friedrich, K. A. Hughen, F. Kaiser, S. Remmele, M. Schaub, and S. Talamo (2004), Late glacial ^{14}C ages from a floating, 1382-ring pine chronology, *Radiocarbon*, *46*(3), 1203–1209.

Lenton, T. M., M. S. Williamson, N. R. Edwards, R. Marsh, A. R. Price, A. J. Ridgwell, J. G. Shepherd, and S. J. Cox (2006), Millennial timescale carbon cycle and climate change in an efficient Earth system model, *Clim. Dyn.*, *26*, 687–711.

Marchal, O., T. F. Stocker, and R. Muscheler (2001), Atmospheric radiocarbon during the Younger Dryas: Production, ventilation, or both?, *Earth Planet. Sci. Lett.*, *185*, 383–395.

McManus, J. F., R. Francois, J.-M. Gherardi, L. D. Keigwin, and S. Brown-Leger (2004), Collapse and rapid resumption of Atlantic meridional circulation linked to deglacial climate changes, *Nature*, *428*, 834–837.

Muscheler, R., J. Beer, G. Wagner, C. Laj, C. Kissel, G. M. Raisbeck, F. Yiou, and P. W. Kubik (2004), Changes in the carbon cycle during the last deglaciation as indicated by the comparison of ^{10}Be and ^{14}C records, *Earth Planet. Sci. Lett.*, *219*, 325–340.

Peltier, W. R. (1994), Ice-age paleotopography, *Science*, *265*, 195–201.

Price, A. R., I. I. Voutchkov, G. E. Pound, N. R. Edwards, T. M. Lenton, and S. J. Cox (2006), Multiobjective tuning of grid-enabled Earth system models using a non-dominated sorting genetic algorithm (NGSA-II), paper presented at 2nd International Conference on e-Science and Grid Computing, Inst. of Electr. and Electron. Eng. Comm. on Scalable Comput., Amsterdam.

Rasmussen, S. O., et al. (2006), A new Greenland ice core chronology for the last glacial termination, *J. Geophys. Res.*, *111*, D06102, doi:10.1029/2005JD006079.

Reimer, P. J., et al. (2004), IntCal04 terrestrial radiocarbon age calibration, 0–26 cal kyr BP, *Radiocarbon*, *46*(3), 1029–1058.

Ridgwell, A., and J. C. Hargreaves (2007), Regulation of atmospheric CO_2 by deep-sea sediments in an Earth system model, *Global Biogeochem. Cycles*, *21*, GB2008, doi:10.1029/2006GB002764.

Ridgwell, A. J., J. C. Hargreaves, N. R. Edwards, J. D. Annan, T. M. Lenton, R. Marsh, A. Yool, and A. Watson (2007), Marine geochemical data assimilation in an efficient Earth system model of global biogeochemical cycling, *Biogeosciences*, *4*, 87–104.

Tarasov, L., and W. R. Peltier (2005), Arctic freshwater forcing of the Younger Dryas cold reversal, *Nature*, *435*, 662–665.

Trenberth, K., J. Olson, and W. Large (1989), A global ocean wind stress climatology based on ECMWF analyses, *Tech. Note NCAR/TN-338+STR,* Natl. Cent. for Atmos. Res., Boulder, Colo.

W. E. N. Austin, School of Geography and Geosciences, St. Andrews University, Irvine Building, North Street, St. Andrews KY16 9AL, UK.

J. W. Beck, NSF-AMS Laboratory, Department of Physics, University of Arizona, Tucson, AZ 85721, USA.

D. A. Richards, A. Ridgwell, J. S. Singarayer, and P. J. Valdes, School of Geographical Sciences, University of Bristol, University Road, Bristol BS8 1SS, UK. (joy.singarayer@bris.ac.uk)